Can We Reach Tbit/sq.in. Storage Densities With Phase-Change Media?

C D Wright, M M Aziz, M Armand, S Senkader and W Yu
Department of Engineering, University of Exeter, UK

ABSTRACT

This paper discusses a number of modelling approaches to simulate phase-transition behaviour in $Ge_2Sb_2Te_5$ material used in optical and electrical phase-change memories. Such models include the well-known Johnson-Mehl-Avrami-Kolmogorov (JMAK) formalism to calculate the fraction of crystallized material. In the literature this model is widely used, but parameters of the model reported by different investigators vary considerably, and can probably be attributed to the inappropriate use of the JMAK approach. In order to overcome the restrictions imposed by JMAK theory, generalizations based on the classical nucleation theory have been suggested and used by several researchers. A more recent alternative modelling technique is the so-called Cellular Automata (CA) approach. A CA representation can be driven by stochastic or deterministic rules, by theoretical descriptions or by empirical rules derived from experimental observations. Finally, yet another approach is that based on evaluating the population density of 'crystal clusters' using rate-equations. Although it is computationally quite intensive, this technique has yielded favourable and reliable results, and we present various simulation-experiment comparisons to illustrate the capabilities of this approach. We also use the various models to assess the limits of thermodynamic stability in GeSbTe phase-change materials, with a view to using such material in ultra-high density (1 Tbit/sq.in. and beyond) scanning probe-based memories. Some write-read simulations of such a memory at Tbit/sq.in densities are also presented.

1. INTRODUCTION

During the last decade there has been great interest in chalcogenide materials, such as GeSbTe or AgInSbTe alloys, for a range of data storage applications. The most prominent and widespread use is of course in the rewritable phase-change optical memory disks, such as CD-RW and the rewritable DVD formats [1,2]. Their use in non-volatile, solid-state, electrical memories, the so-called OUM (Ovonic Unified Memory) or PC-RAM (Phase-Change RAM), is also generating much interest as they offer a possible replacement for conventional CMOS flash memory [3,4]. The use of phase-change materials for scanning probe based memories, similar in concept to the well-known IBM Millipede system [5,6], has also gained attention recently. All of these memory applications rely on a reversible phase transformation of the chalcogenide based alloy between the amorphous and (poly)crystalline states. In optical disk memories such phase-transformations are brought about by heating from a focused laser to transform from crystalline to amorphous (and back); readout relies on the differing optical reflectivities of the two phases. In electrical phase-change memory devices, data is written or erased by resistive heating caused by a pulse of electrical current injected into the phase-change layer (this is true also for the scanning probe type phase-change memory in [5,6]); readout relies on the differing electrical resistivities of the two phases which can be more than three-orders-of-magnitude.

Thus, it is clear that phase-change materials may find use in many different memory architectures, and it is desirable to have a thorough understanding of the physical processes involved in such applications. Furthermore, direct experimental investigation of the phase-transition process is often difficult, since in real applications transitions occur on short time-scales (tens to hundreds of nanoseconds) and on short-length scales (tens to hundreds of nanometres). Theoretical modelling can, and does, therefore play a major role in describing memory performance and designing future systems.

2. MODELS FOR CRYSTALLIZATION IN PHASE-CHANGE ALLOYS

In general the recording process in phase-change memories is a complicated one, and the size and shape of the recorded mark depends on the detail of the electrical and thermal fields present in the recording layer, the media structure and material properties, including phase-transition kinetics. Methods for calculating the electrical and thermal fields are quite mature, and typically use finite difference time domain (FDTD) and/or finite element methods (FEM) to solve Maxwell's equations and the heat diffusion equation throughout the region of interest. Accurate approaches to modelling the phase-change process itself are however less certain.

Traditional approaches to modelling crystallization in phase-change materials used for data storage applications fall essentially into two categories; those based on Johnson-Mehl-Avrami-Kolmogorov (JMAK) theory [7-11], and those based on classical nucleation theory [12-15]. JMAK theory allows calculation of the volume fraction of crystallized material, while classical nucleation theory provides a means to estimate the cluster nucleation and growth rates, and crystallite size distributions. Both theories have inevitable limitations, which should be recognized.

2.1 JMAK Theory

The volume fraction of the transformed material, x, under isothermal annealing conditions is described by the well-known JMAK equation

$$x(t) = 1 - \exp[-(k\ t)^n] \qquad (1)$$

where t is time, n is the Avrami coefficient and k is an effective rate constant. Theoretically the Avrami coefficient should be an integer providing information on the dimensionality of the crystallization process. The effective rate constant describing the nucleation and growth rates is generally given by an Arrhenius equation

$$k(T) = \nu \exp\left(-\frac{E_A}{k_B T}\right) \qquad (2)$$

where ν is the frequency factor, E_A is the activation energy, T is the absolute temperature and k_B is the Boltzmann constant. When JMAK theory is applied to the analysis of GST material, the reported activation energies are generally around 2 *eV,* but some values are as low as 0.81eV [16] and some as high as 3eV[17]. There are fewer reported values for the Avrami coefficient, n, and they are less consistent ranging from 2.5 [18] to 5.8 [19]. While the discrepancies in reported n values are bad enough it becomes worse when we turn to the frequency factor ν, which varies between 10^{17} and 10^{86} s^{-1} [18, 20, 21]. The variation of reported JMAK parameters is no doubt a result of the limitations of the JMAK model itself. In the original formalism for the JMAK model, for example, several assumptions were made, namely: 1) nucleation occurs randomly and uniformly, 2) the nucleation rate is time-independent, 3) the growth rate is size independent, and 4) growth is interface controlled. Such assumptions are clearly not valid in many cases, including those pertaining to data storage. Of course JMAK theory has been extended and enhanced by several authors [22,23] to include studies of transient effects, non-uniform nucleation, anisotropic particle formation, non-isothermal treatments etc. Such theories are useful in understanding and predicting crystallisation behaviour for data storage applications [24].

2.2 Classical Nucleation Theory

Classical nucleation theory in its original form [12] has several limitations, including the requirement for isothermal, steady-state conditions. Again, extensions of the formalism to include transient effects and non-isothermal conditions mean that such theory [25] is more useful in terms of modelling recording behaviour in phase-change memories, and indeed several authors have adopted this approach recently in the study of advanced optical recording formats [18, 26, 27]. According to classical nucleation theory, the steady-state nucleation rate, I^{ss}, may be expressed as:

$$I^{ss} = 4\ f(1)\ \gamma\ n_c^{2/3}\ Z \exp\left(-\frac{\Delta G_c}{k_B\ T}\right) \qquad (3)$$

where n_c is critical cluster size (in number of GST monomers), γ is the molecular jump frequency, Z is the Zeldovich factor, $f(1)$ is the concentration of GST 'monomers', ΔG_c is the free energy required to form a nucleus of critical radius (for a fuller description of these terms see for example [25 or 28]). Nucleation rate in $Ge_2Sb_2Te_5$ according to Eq(3) is shown in Fig. 1. In practice this steady-state nucleation rate is reached after a certain incubation time and, as already mentioned, GST shows substantial incubation times during crystallization. Therefore transient effects should be taken into account for realistic calculations of the nucleation rate. An analytical treatment of transient effects is given by Kashchiev [29] who proposed the nucleation rate for isothermal annealing conditions to be

$$I(t) = I^{ss}\left(\frac{4\ \pi\ \tau}{t}\right)^{1/2} \exp\left(-\frac{\pi^2\ \tau}{4\ t}\right), \qquad \text{where} \quad \tau = \frac{1}{\pi^3\ n_c^{2/3}\ \gamma\ Z^2} \qquad (4)$$

where τ is incubation time. The effect of incubation time on the nucleation rate is shown in Fig. 2; it can be seen that (at 250^0C) ~2 ms is required to reach the steady-state. This incubation time is much larger than the operating times used in memory devices suggesting that the whole crystallization process might be in the transient regime.

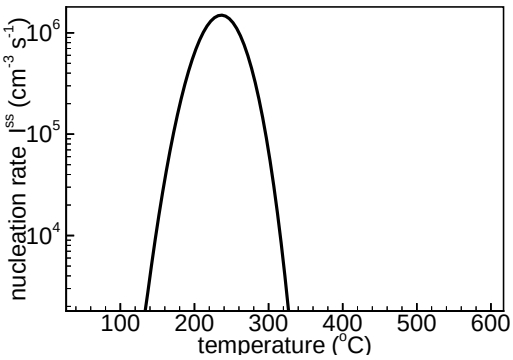

Fig 1 Nucleation rate vs temperature for GST (σ=0.1Jm^{-2},T_m=900K, ΔH_f = 625 Jcm^{-3}, f(1) =3.44x10^{27} m^{-3})

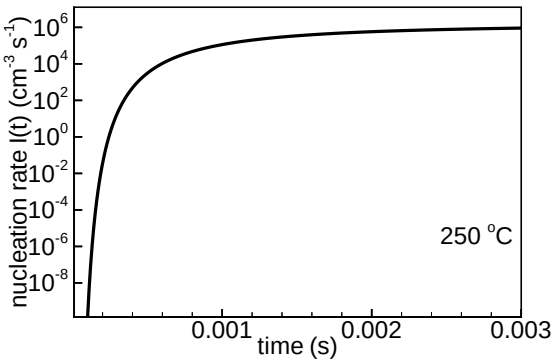

Fig 2 Nucleation rate vs time at 250^{0}C for GST

Once nucleated crystalline clusters grow by the attachment of GST monomers. A common description [26,27,30] of the growth rate is given by:

$$V_g = V_o \exp(-E_{ag} / k_B T)(1 - \exp(-\Delta g / k_B T)) \qquad (5)$$

where V_o is an 'attempt' growth-velocity prefactor, E_{ag} is a growth activation energy term, Δg is the bulk free energy difference per GST monomer between the two phases, which, using the approximation of Singh and Holz [31], is

$$\frac{\Delta g}{v_m} = \Delta H_f \frac{T_m - T}{T_m}\left[\frac{7\,T}{T_m + 6\,T}\right] \qquad (6)$$

where T_m is the melting temperature, ΔH_f is the enthalpy of fusion at melting point and v_m is the volume of a GST monomer. Growth behaviour described by Eqs.(5) and (6) is shown for GST in Fig. 3, and implicitly assumes that crystal clusters of all sizes grow at the same rate, which of course in reality is not true. Kelton and Greer [32] addressed this issue to find the average growth rate of a cluster of radius r as

$$\frac{dr}{dt} = \frac{16\,D}{\pi^2}\left(\frac{3\,v_m}{4\,\pi}\right)^{1/3} \sinh\left[\frac{1}{2\,k_B\,T}\left(\Delta g - \frac{2\,\sigma}{r} v_m\right)\right] \qquad (7)$$

where D is the diffusion coefficient and σ is the interfacial energy density. Growth rates according to Eq.(7) are shown in Fig. 4, where it is clear that the maximum growth rate occurs at different temperatures for different cluster sizes.

While the above approaches can be very useful in guiding our understanding of phase-transition processes, it is clear that they rely on many, sometimes physically unrealistic, assumptions and approximations. In particular we note that the simulation of optical and electrical phase-change memory devices demands the handling of nucleation and growth in very short time scales, where the crystallization process is determined largely by transient and non-equilibrium conditions. It is therefore helpful to examine models that can treat the nucleation and the growth simultaneously and consider transient effects fully. One possible approach is that based on rate-equations.

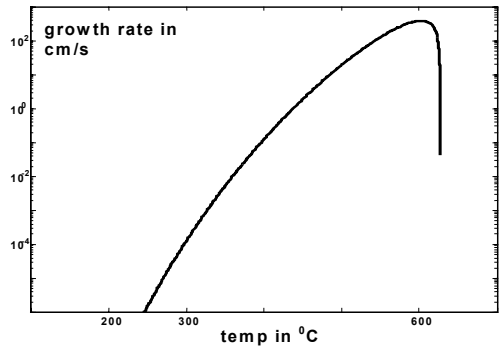

Fig 3 Growth rate vs temperature for GST (V_0=2x10^{14}, E_{ag} = 2.3eV)

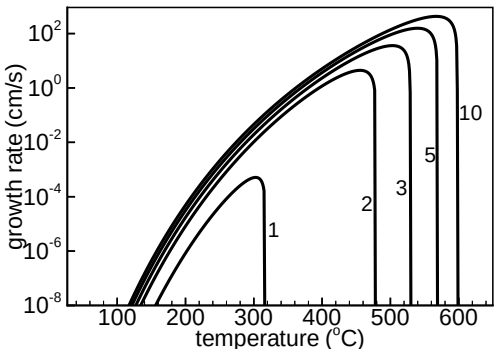

Fig 4 Growth rate vs temperature for different cluster sizes (n is number of GST monomers in cluster, D= $\gamma\lambda^2$ where λ is interatomic distance ~ 0.3nm)

2.3 The Rate-Equation Method

The rate-equation method considers that during nucleation in a real system there will be not only crystalline clusters of critical size but a distribution of clusters of different sizes. These clusters will interact with each other and this interaction will establish the progress of the crystallization process. Therefore, instead of considering only clusters of critical size we might take into account both subcritical and supercritical clusters and establish the resulting cluster size population density, which is of course directly related to the crystallised fraction. Considering that the smallest possible cluster size is two GST monomers, i.e., a GST dimer, and assuming the interactions among different sizes to be through monomers at a given time, a cluster can gain or lose a GST monomer to grow or dissolve, respectively. According to this schema we can write a continuity equation for each cluster size and the concentration *f(n,t)* of clusters of size *(n)* is

$$\frac{\partial f(n,t)}{\partial t} = g(n-1,t)f(n-1,t) - d(n,t)f(n,t) - g(n,t)f(n,t) + d(n+1,t)f(n+1,t) \quad ; \quad n\geq 2 \qquad (8)$$

where *g(n,t)* and *d(n,t)* are the growth and dissolution rates of size *(n)*, respectively. To solve the set of rate equations given by Eq. (8) one needs to determine the growth and dissolution rates. We modelled them following the work of Turnbull and Fisher [15] and using the theory of reaction rates [33] as

$$g(n,t) = 4\pi r^2 \lambda f(1,t)\gamma \exp\left(-\frac{\Delta G_{n\to n+1}}{2kT}\right), \qquad (9)$$

$$d(n+1,t) = 4\pi r^2 \lambda f(1,t)\gamma \exp\left(\frac{\Delta G_{n+1\to n}}{2kT}\right) \qquad (10)$$

where *f(1,t)* is the concentration of GST monomers at a given time. The energy terms in the Boltzmann factors have been defined as Gibbs free energy differences between sizes *(n)* and *(n+1)* such that

$$\Delta G_{n\to n+1} = \Delta G(n+1,t) - \Delta G(n,t), \quad \text{where} \quad \Delta G = 4\pi r^2\sigma - n\Delta g \qquad (11)$$

The solution of the set of equations given by Eq.(8) yields the size distribution function of crystalline clusters of GST. A typical solution, for two different heating regimes, is shown in Fig. 5. It can be seen that the population of cluster sizes varies greatly for different thermal treatments. In order to find experimentally observable quantities, such as the fraction of crystallized material we integrate the population density distribution function, taking into account that available amorphous material for crystallization is continuously depleted, i.e., conservation of matter dictates that

$$f(1,t) = f(1,0) - \int_2^{n_{\max}} f(n,t)\, dn \qquad (12)$$

We have used the rate-equation model to compare predictions of this simulation approach to previously published experimental results. We have found excellent agreement for a wide range of thermal treatments, for a variety of GST compositions and for a variety of substrate/GST layer combinations [28,6,34]. As an example, we show in Fig. 6 a comparison of the rate-equation simulation results to a 'DC' plus ramped annealing experiment for $Ge_2Sb_2Te_5$ on silicon [35]. The agreement is very good with only two fitting parameters - the interfacial energy and a geometric factor from the 'spherical cap' model used to mimic the effect of the different wetability of different substrates.

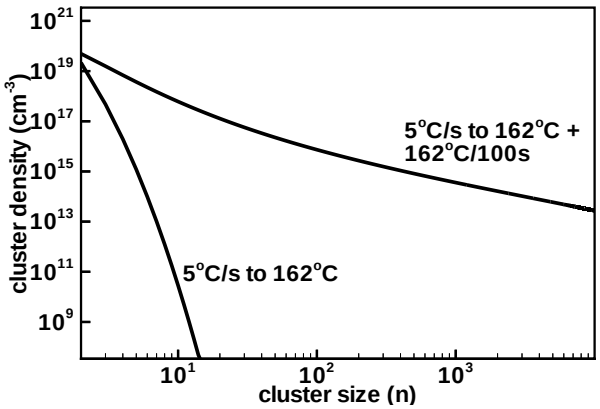

Fig 5 Predicted population density of clusters for two different thermal treatments

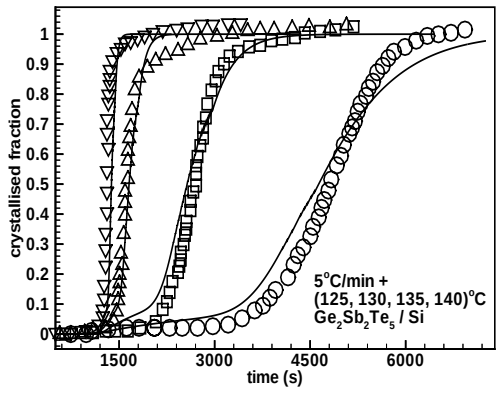

Fig 6 Comparison of theory (lines) and experimental results from [35] (circles) for crystallisation studies of GST

2.3 The Cellular Automaton (CA) Method

An approach that does not seem to have so far been used to model the phase-change process in data storage applications is the so-called Cellular Automaton (CA) method [36]. A CA is an algorithm that describes the discrete spatial and/or temporal evolution of a complex system by applying local deterministic or probabilistic transformation rules to the cells of that system. Each cell is characterised by different states (e.g. temperature, orientation, colour,..), and by taking into account the states of cells in its neighbourhood, the state of an individual cell can be made to change by time-stepping according to a transition rule**.** The transition rules are the most important part in the CA model, and determine the state of a cell as a function of its previous state and the state of its neighbouring cells. The CA approach has several attractions when considered as a possible means with which to model recording processes in phase-change storage media. Firstly, it is fairly straightforward to couple the CA lattice to thermal and electrical simulation spaces from FDTD or FEM calculations. Secondly, the CA model reveals the local microstructure (rather than for example just giving a volume fraction of crystallised material), and can thus yield detailed information on the size and shape of written bits. Thirdly, the CA transition rules themselves are inherently flexible; they can be deterministic or probabilistic, so can be used to implement closed form analytic descriptions of crystallization behaviour (if so desired), or follow an entirely probablistic route derived from, for example, a set of experimental (microstructural) observations of crystallisation. Finally, the CA model is relatively straightforward to implement in code and can run with modest computing power, e.g. an IBM-type PC. Fuller details about our CA method and have been given elsewhere [37].

In order to simulate the above nucleation and growth processes, according to the basic requirement of the CA method, a network of cells is laid out to construct a regular lattice arrangement in which the distance between two neighbouring cells is arbitrarily assumed to be 1 CA distance unit. In the model used here the lattice was made up from a 400×400 regular network of cells with a periodic boundary condition. The state of each cell in the lattice is defined by a state-index, initially set to zero. During each time step, all cells with index zero are scanned and a random number (p) generated for each of them ($0<p<1$). Nucleation within a cell is deemed to occur if p is smaller than the nucleation probability P_n. At this time, the cell index is changed to a positive integer (chosen randomly in range 1 to Q), which represents the orientation of the crystallite grain in the simulated microstructure. At the same time, cells with a nonzero state-index have a chance to consume neighbouring cells with index zero. There is a probability P_g for such a transformation. Those cells consumed are assigned the same index as the consuming nuclei; this process reflects the crystal growth. These processes continue until no cell with a zero state-index exists in the lattice. At this time, grain shapes will be irregular and different in size, and grain orientations different. After this stage, grain growth dominates since all cells either contain a nucleus or have already been 'grown into' (consumed) by an adjacent cell. The CA model can reveal the resulting microstructure for a wide range of thermal treatments and for a wide variety of crystallization behaviours. In Fig. 7 we show a simple example of nucleation and growth probabilities on the resultant microstructure for an isothermal annealing treatment.

There are of course limitations with the CA approach, as with most modelling techniques. The behaviour of individual cells is governed by the CA transition rules; if these rules are unrealistic the simulations will generate unrealistic results. The beauty of the CA method however is that the transition rules can be easily adapted and modified to take account of new theoretical insights or experimental observations, tailoring the model so that it more accurately predicts the behaviour of the system under consideration.

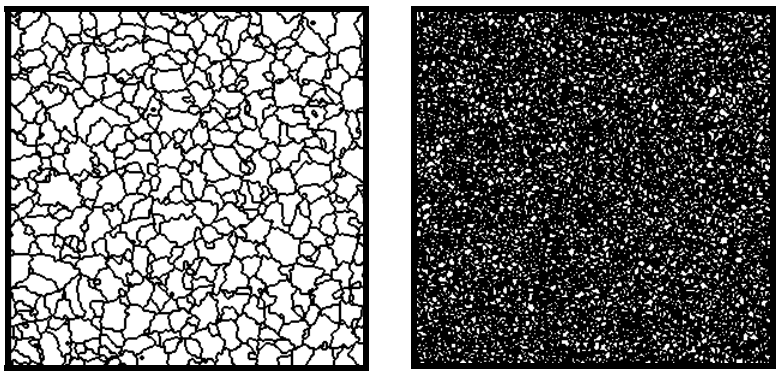

Fig. 7 CA model predictions of grain structure in growth dominant material (left, $P_g = 0.1$, $P_n = 0.0001$) and nucleation dominant material (right, $P_g = 0.01$, $P_n = 0.001$). Temperature assumed constant.

3. TERABIT/SQ.IN STORAGE WITH PHASE-CHANGE MATERIALS

It is common knowledge that data storage industry roadmaps are currently looking towards areal density targets of 1Tbit/sq.in. by around 2008-2010. For magnetic-based recording, because of the well-known superparamagnetic 'limit', such a target requires significant research and development both in terms of storage materials (ultra high anisotropy, very low grain size dispersion) and system design (e.g. heat-assisted recording heads). A question often asked is 'do phase-change materials suffer from an equivalent to the superparamagnetic limit?'. We can go someway towards answering this question using the theoretical models presented above. For example, a first step would be to use classical nucleation theory to evaluate the minimum stable crystallite cluster size (n_c) as a function of temperature; this is shown in Fig. 8, where it can be seen that sizes of the order 1nm to 5nm are stable over the typical operating temperatures of phase-change storage media. Assuming such small bits can be written, we can estimate their longevity by inspection of predicted growth rates (for crystalline bits written in an amorphous background) and incubation times (for amorphous bits written in a crystalline background) with the aid of Eqs (4) and (5). Growth rate for GST has already been shown in Fig. 3, and incubation time is shown in Fig. 9. Clearly, the theory predicts that growth rates at room temperature are extremely low, and incubation times extremely long, so that nanometric bits in both crystalline and amorphous phases of GST are predicted to be thermodynamically stable for very long times at room temperature.

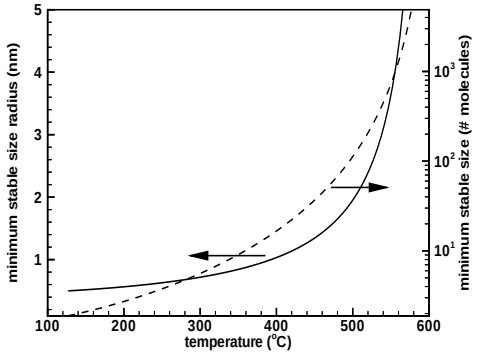

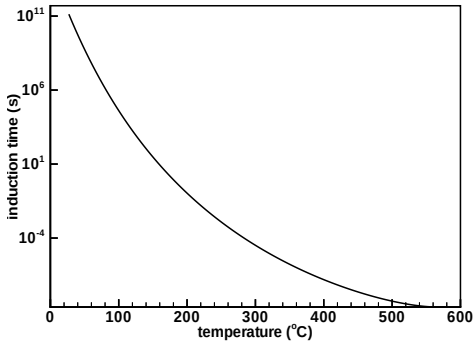

Fig. 8 (left) Minimum stable cluster size for $Ge_2Sb_2Te_5$ vs temp

Fig 9 (right) Incubation time for onset of crystallisation vs temp.

Since nanometric-sized bits are predicted to be stable in phase-change materials, the next question to address is how such bits might be written and read. One possible approach is via scanning probe techniques. As part of an EU Framework V funded research project in collaboration with partners at LETI-CEA in Grenoble, and the University of Twente, we are developing such a phase-change based scanning probe memory. In our approach, illustrated in Fig. 10 bits are written by injecting current from an electrically conducting AFM-type tip into the recording medium, thereby heating it. Readout is by sensing the differing electrical resistance of the amorphous and crystalline phases.

In order to simulate the recording and readout processes of such a memory, it is necessary to develop suitable electrical and thermal models that can be combined with the phase-change models described above. We used a system of coupled equations defined by the Laplace and the heat diffusion equations

$$\nabla.\left(\vartheta.\nabla\Phi\right)=0 \qquad (13) \qquad ; \qquad \rho C_p \frac{\partial T}{\partial t} - K.\nabla^2 T = \vartheta\left|\xi\right|^2 \qquad (14)$$

where ϑ is the electrical conductivity, Φ is the electrical potential, ξ is the electric field and ρ, K, and C_p correspond to the density, the thermal conductivity and the specific heat, respectively. The amorphous and the crystalline states of $Ge_2Sb_2Te_5$ have of course different electrical and thermal conductivities, and conductivity itself can be a strong function of temperature. In addition, it is well-known that in the amorphous state the electrical conductivity of chalcogenide-type materials can depend strongly on the applied electrical field. Thus, we represent the electrical conductivity of amorphous and crystalline phases as

$$\vartheta_{am}\left(T,\xi\right)=\vartheta_{0am}\exp\left(-\frac{E_{am}}{k_B T}\right)\times\exp\left(\frac{\xi}{\xi_0}\right), (15) \; ; \quad \vartheta_{cryst}\left(T\right)=\vartheta_{0cryst}\exp\left(-\frac{E_{cryst}}{k_B T}\right) \; \Omega^{-1}\mathrm{m}^{-1} \quad (16)$$

where ϑ_{0am} and ϑ_{0cryst} are constants, E_{am} and E_{cryst} are the activation energies for the conductivity temperature dependencies and ξ_0 is a critical electric field. Within this theoretical framework, we examined the writing of crystalline

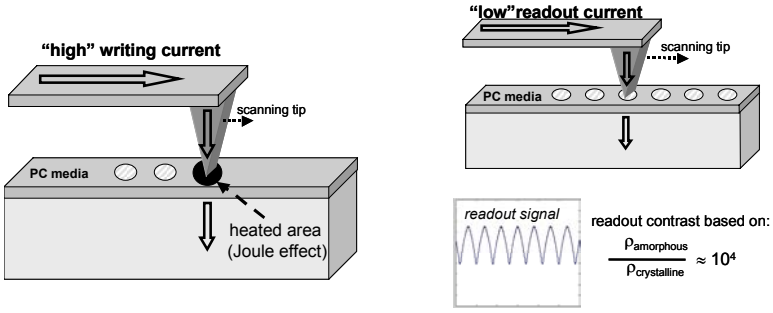

Fig. 10 Schematic of electro-thermal write and electrical read processes for proposed probe storage using phase-change media

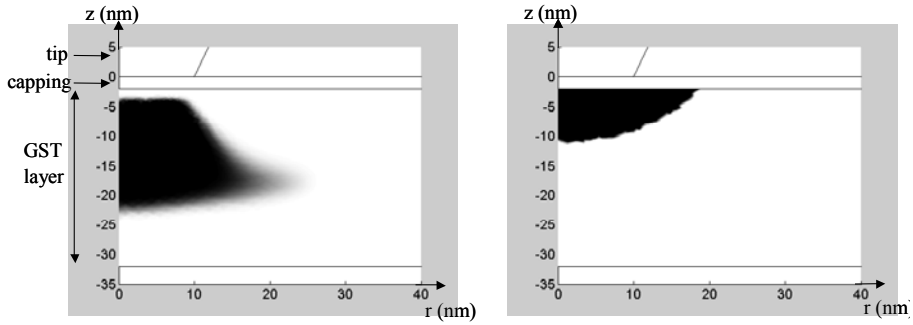

a) Crystalline dot b) Amorphous dot

Fig. 11 Simulated recorded bits in media stack comprising capping layer, GST layer, underlayer, silicon. (a) is crystalline bit in amorphous background; (b) is amorphous bit in crystalline background. A 10V (a) or 15V (b) 200ns write pulse was applied. ($\vartheta_{0am} = 1.9\text{x}10^4\ \Omega^{-1}\text{m}^{-1}$, $\vartheta_{0cryst} = 1.5\text{x}10^4\ \Omega^{-1}\text{m}^{-1}$, $E_{am} = 0.3$eV, $E_{cryst}=0.04$eV, $\xi_0=5\text{x}10^7\ \text{Vm}^{-1}$)

bits in an amorphous background, and vice-versa. Typical results are shown in Fig. 11. The different location and size of the crystalline and amorphous bits reflects the different temperature profiles in the two cases. In both configurations, the writing process is characterised by a very low power consumption, and this represents one of the major advantages of this probe storage technique. Indeed, only 106pJ and 364pJ respectively were needed to write the crystalline and amorphous dots in Fig. 11.

To study the readout process theoretically we assume idealized bit structures, as shown in Fig. 12, representing the actual shapes predicted in our recording simulations above. In addition, to maintain computational tractability, we limited the readout study to two dimensions such that the results are equivalent to scanning an infinitely wide tip over a bit of infinite width. The size of the dots in each case was 20nm, and constant electrical conductivities of $1000\Omega^{-1}\text{m}^{-1}$ and $0.1\Omega^{-1}\text{m}^{-1}$ for the crystalline and the amorphous states respectively were assumed. A voltage of 4V was applied between the tip and the active structure. The calculated readout signals are plotted in Fig. 12(b). The three signals exhibit different levels of readout current depending on the relative proportion of crystalline and amorphous material, but are here shown normalised. A parameter that may be used to characterise the readout process is the contrast $(I_{max} - I_{min})/(I_{max}+I_{min})$, in which case the three configurations present a readout contrast of 0.05, 0.97 and 0.5 respectively. In a real system the readout performance is of course best measured by the signal to noise ratio, but so far we have not examined the noise processes in this new type of memory.

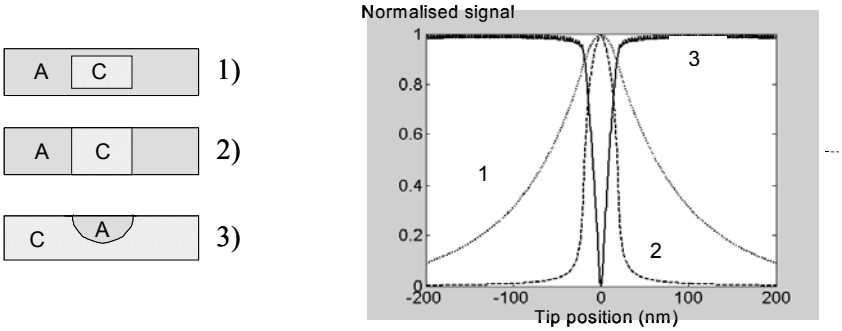

Fig. 12 Idealised bit structures (left) used in readout modelling; normalised readout signals (current) for the three idealised cases. Width of each dot in simulation is 20nm. Constant voltage of 4V applied

4. CONCLUSIONS

We have presented various approaches to modelling phase-transition processes in phase-change storage materials, outlining their possible limitations and areas of applicability. JMAK theory offers the simplest approach to modelling, but is compromised in non-isothermal, transient and heterogeneous conditions, all of which are usually present in data storage applications. Classical nucleation and growth theory can be used with good effect to model phase-change behaviour, including the important data storage write and read processes. A more rigorous approach may be given by rate-equation models, which we have shown capable of matching very well a wide range of published experimental crystallisation data from a large number of different sources. The rate-equation method is computationally intensive, and so at present we have not been able to use this approach to model both temporal and spatial behaviour simultaneously. However, we continue to develop this approach and expect improvements soon. Yet another modelling method that does not so far seem to have been used in the data storage arena is the Cellular Automata approach. Some preliminary studies using this CA method have been presented. Using the various models we have shown that very small, nano-scale, crystallites are predicted to be thermodynamically stable in GST. A possible method for writing and reading such nano-scale bits has been presented and uses electro-thermal writing and electrical reading in a phase-change medium addressed by an electrically conducting AFM-type tip.

Acknowledgements
The authors acknowledge the support of the EU Framework 5 programme in supporting this work under the auspices of the InProM and PC-RAM projects (IST-2001-33065 and IST-2001-32557).

References

[1] Libera M. and Chen M. MRS Bulletin 1990;15: 40.
[2] Yamada N. et al. J. Appl. Phys. 1991;**69**:2849.
[3] Ovshinsky S.R, and Noncryst J. Solids 1970; **2**: 99.
[4] Gill M., Lowrey T., and Park J. Proceedings of 2002 IEEE International Solid State Circuits Conference , 2002.
[5] Gotoh T et al, Jpn J Appl Phys,2004 , **3,** L818
[6] Wright C.D et al, Mat Res Soc Symp Proc, 2004, **803**, 61
[7] Johnson WA and Mehl RF, Trans. AIME 1939; **135**: 416 .
[8] Avrami M. J. Chem. Phys. 1939 ;**7** : 1103.
[9] Avrami M. J. Chem. Phys. 1940 ; **8** : 212 .
[10] Avrami M. J. Chem. Phys. 1941; **9**: 177 .
[11] *Selected Works of A. N. Kolmogorov,* edited by A. N. Shiryayev (Kluwer Academic, Dordrecht, 1992).
[12] Volmer M. and Weber A. Z. Phys. Chem. 1926;**119**: 227 .
[13] Becker R. and Döring W. Ann. Phys. (Leipzig) 1935; **24**: 719 .
[14] Frenkel J. *Kinetic Theory of Liquids* , Oxford University Press, Oxford, 1946.
[15] Turnbull D.and Fisher JC, J. Chem Phys. 1949;**17**: 71
[16] Trappe C et al, Jpn J Appl Phys, 2000, Part 1 **2B**, 766
[17] Tominaga J et al, Jpn J Appl Phys, 1998, Part 1, **37**, 1852
[18] Weidenhof et al, J Appl Phys, 2001, **89**, 3168
[19] Jeong T H et al, J Appl Phys, 1999, **86**, 774
[20] Ruitenberg G et al, J Appl Phys, 2002, **92**, 3116
[21] Trappe C et al, Jpn J Appl Phys, 1998, Part 1, **4B**, 2114
[22] Weinberg MC, Birnie III DP and Shneidman VA. J Non-Crystalline Solids, 1997; **219**: 89
[23] Weinberg MC and Birnie III DP. J Non-Crystalline Solids, 1996; **202**: 290 .
[24] Nishi Y., Kando H. and Terao M. SPIE Proceedings, 2002;**4342**:88 .
[25] Kelton KF, Greer AL and Thompson CV, J Chem Phys, 1983;**79**: 6261.
[26] Hyot B., Rolland B., Fargeix A. et al, J.Magn.Soc.Japan, 2001;**25**: 414.
[27] Meinders et al, J Appl Phys, 2002, **91**, 9794
[28] Senkader S and Wright C D, J Appl Phys, 2004, **95,** 504
[29] Kashchiev D, Surf Sci, 1969, **14**, 209
[30] Martens H C F et al, J Appl Phys, 2004, **95**, 3977
[31] Singh H B and Holz A, Solid State Commun, 1983, **45**, 985
[32] Kelton K F and Greer A L, J Non-Cryst Sol, 1986, **79**, 295
[33] Christian J W, *The Theory of Transformations in Metals and Alloys*, Pergamon Press, Oxford, 1975
[34] Senkader S et al, SPIE Proceedings, 2003, **5069**, 98
[35] Weidenhof V, PhD Thesis, Forshungzentrum Julich, Jul-3787, 2000
[36] D.Raabe, *Computational Materials Science*, Wiley-VCH , 1998.
[37] Yu W., Wright CD, Banks SP and Palmiere EJ. IEE Proceedings, Sci. Meas. Technol., 2003;**150**: 211.